Dynamic Performance Analysis of Self-commutating PWM CSI-fed Induction Motor Drive under MATLAB Environment

S. M. Tripathi [1] A. K. Pandey [2]

Abstract–In this paper, an attempt has been made to investigate analytically the dynamic performance of self-commutating current source inverter-fed induction motor drive with volts/Hz control strategy. Speed and current PI regulators are used in realization of closed loop control structure of the drive system. The closed loop mathematical modeling of the complete drive system is presented in the synchronously rotating d^e-q^e reference frame. The dynamic performance curves of the drive are obtained through MATLAB simulation and are discussed in detail.

Keywords–Current source inverter, induction motor drive, pulse width modulation (PWM), dynamic performance, V/f control.

NOMENCLATURE

d, q	Direct and quadrature axes
v_{as}, v_{bs}, v_{cs}	Phase voltages of the PWM inverter
v_{ds}^e	*d*-axis stator voltage in synchronously rotating reference frame
i_{ds}^e	*d*-axis stator current in synchronous rotating reference frame
v_{qs}^e	*q*-axis stator voltage in synchronously rotating reference frame
i_{qs}^e	*q*-axis stator current in synchronously rotating reference frame
i_{dr}^e	*d*-axis rotor current in synchronously rotating reference frame
i_{qr}^e	*q*-axis rotor current in synchronously rotating reference frame
i_{as}, i_{bs}, i_{cs}	Line currents of PWM inverter
I_{DC}	DC link current
I_{act}	Active component of stator current
I_{act}^*	Reference active component of stator current
I_{react}	Reactive component of stator current
I_{react}^*	Reference reactive component of stator current
ω_e	Switching frequency of the inverter
ω_r	Rotor speed of the induction motor
ω_{ref}	Reference speed
ω_{sl}	Slip speed of the induction motor
ω_{sl}^*	Reference slip speed
I_{ref}	Reference DC link current
V_{inv}	Input voltage of the inverter
V_r	Rectifier output voltage
R_f	Resistance of DC link inductor
L_f	Inductance of DC link inductor
R_s	Resistance of stator winding per phase
L_s	Self-inductance of stator winding per phase
R_r	Resistance of rotor winding per phase
L_r	Self inductance of rotor winding per phase
L_m	Mutual inductance per phase
L_1	$L_s L_r - L_m^2$
C	Capacitance per phase
J	Moment of inertia in kg-m2
B	Viscous friction coefficient
β	Pulse width of PWM rectifier
V_{LL}	Line-to-line input voltage of the rectifier
P	Number of poles
I_c	Instantaneous phase current of capacitor
V_s	Instantaneous stator phase voltage
i_{dc}^e	*d*-axis capacitor current in synchronously rotating reference frame
i_{qc}^e	*q*-axis capacitor current in synchronously rotating reference frame
k_{p_i}	Proportional gain of current regulator
k_{i_i}	Integral gain of current regulator
k_{p_s}	Proportional gain of speed regulator
k_{i_s}	Integral gain of speed regulator
p	Differential operator (d/dt) or complex frequency
k	$\frac{\text{Maximum value of fundamental inverter line current}}{\text{DC link current}}$
k_1	Slope of stator active current (I_{act}) *vs.* slip speed (ω_{sl})
k_2	Slope of stator reactive current vs. slip speed (ω_{sl})
k_{11}	$\frac{\text{Rated value of capacitor current per phase}}{[\text{Rated angular frequency } (\omega_e)]^2}$

I. INTRODUCTION

The speed control of induction motors is possible over a wide range by feeding the motor through variable frequency VSI or CSI. Due to the controlled current operation of the inverter, slip-regulated CSI is preferred over VSI. The current source at the front end makes the system naturally capable of power regeneration [1]–[4]. In this paper, the closed loop scheme of self-commutating current source inverter-fed induction motor drive employing two PI regulators is presented. The selection of parameters for current and speed PI regulators of a self-commutating CSI-fed induction motor drive are made on the basis of system relative stability, frequency scanning, and transient response of the drive, as thoroughly discussed in [5].

II. SYSTEM DESCRIPTION

The CSI-fed induction motor drive consists of a three-phase AC source, a PWM rectifier, a DC link smoothening reactor, a current-controlled inverter, a three-phase squirrel cage induction motor, and a three-phase capacitor bank, as shown in Figure 1. A fast-response speed-

The paper first received 3rd Jan 2011 and in revised form 20th May 2011.
Digital Ref: A190711101

[1] Department of Electrical Engineering, Kamla Nehru Institute of Technology, Sultanpur (U.P.), India, E-mail: mani_excel@yahoo.co.in
[2] Department of Electrical Engineering, M. M. M. Engineering College, Gorakhpur (U.P.), India, E-mail: akp1234@gmail.com

regulating drive can be realized by incorporating PI regulators in the feedback loops [6]–[9]. Two PI regulators are used – one in the speed feedback loop and the other in the current feedback loop. The outer speed regulator compares the reference speed and the actual rotor speed and processes the speed error to obtain the reference slip speed (ω_{sl}^*) which is required to estimate the reference stator active current (I_{act}^*) and reference stator reactive current (I_{react}^*) of the induction motor and hence, reference DC link current (I_{ref}). It is also used in the calculation of switching frequency (ω_e) of the inverter. The following mathematical equations are used:

$$\omega_{sl}^* = \left(k_{p_s} + \frac{k_{i_s}}{p} \right) (\omega_{ref} - \omega_r) \tag{1}$$

$$I_{act}^* = k_1 \, \omega_{sl}^* + \text{constant} \tag{2}$$

$$I_{react}^* = k_2 \, \omega_{sl}^* + \text{constant} \tag{3}$$

$$\omega_e = \omega_r + \omega_{sl}^* \tag{4}$$

The current PI regulator is used to regulate the error between the reference DC link current and actual DC link current. The output of current PI regulator decides the pulse widths of the PWM rectifier pulses and hence, controls the output voltage of the pulse width modulated rectifier, which in turn controls the DC link current. The output voltage of the rectifier in terms of current regulator parameters is given by the following expression:

$$V_r = \left(k_{p_i} + \frac{k_{i_i}}{p} \right) (I_{ref} - I_{DC}) \tag{5}$$

The reference DC link current is determined using the equation:

$$I_{ref} = \left(\sqrt{\left(I_{act}^*\right)^2 + \left(I_{react}^* - I_{c'}\right)^2} \right) . \left(\frac{\sqrt{2}}{k} \right) \tag{6}$$

For the V/f control operation of the drive I_c may be expressed as

$$I_c = k_{11} \, \omega_e^{\,2} \tag{7}$$

where, $k_{11} = \dfrac{I_{c\,(rated)}}{(\omega_{e\,(rated)})^2}$

III. Mathematical Model of the Drive

The modeling of the PWM CSI-fed induction motor drive is carried out in synchronously rotating reference frame for the following:

A. Three-phase PWM rectifier
B. Three-phase PWM inverter
C. DC link
D. Three-phase induction motor with load
E. Three-phase capacitor bank

A. Three-phase PWM rectifier

The PWM rectifier output voltage depends on the number of pulses per cycle and their widths. The converter is modeled for twelve numbers of equal pulses per cycle. It leads to two pulses per 60° each of β width. The average output voltage of the PWM rectifier can be expressed as follows:

$$V_r = \frac{3\sqrt{2}}{\pi} V_{LL} \left(4 \sin \frac{5\pi}{12} \right) \sin \frac{\beta}{2} \tag{8}$$

Since β is varied from 10% to 90% of (π/6) radians, hence, (β/2) is very small and it can be approximated as follows: sin (β/2) ≅ (β/2). Therefore,

$$V_r = 5.218 \, V_{LL} \, (\beta / 2) \tag{9}$$

B. Three-phase PWM inverter

The fundamental component of the line currents of the three-phase pulse width modulated inverter i_{as}, i_{bs}, and i_{cs} forms a balanced set of three-phase currents with maximum value as $I_{as(max)}$ and can be expressed as follows:

$$I_{as\,(\max)} = k I_{DC} \tag{10}$$

where, k is obtained through Fourier analysis of inverter line current waveforms, and this is given by the following:

$$k = \frac{\text{maximum value of fundamental inverter line current}}{\text{DC link current } (I_{DC})}$$

The value of k depends on the operating frequency of the inverter and varies from 0.8485 to 0.9970 for variation in operating frequencies from 10 to 50 Hz. Since the inverter output fundamental current peak is taken along the q^e axis of the reference frame, the transformed phase current equations in the d^e-q^e reference frame are as follows:

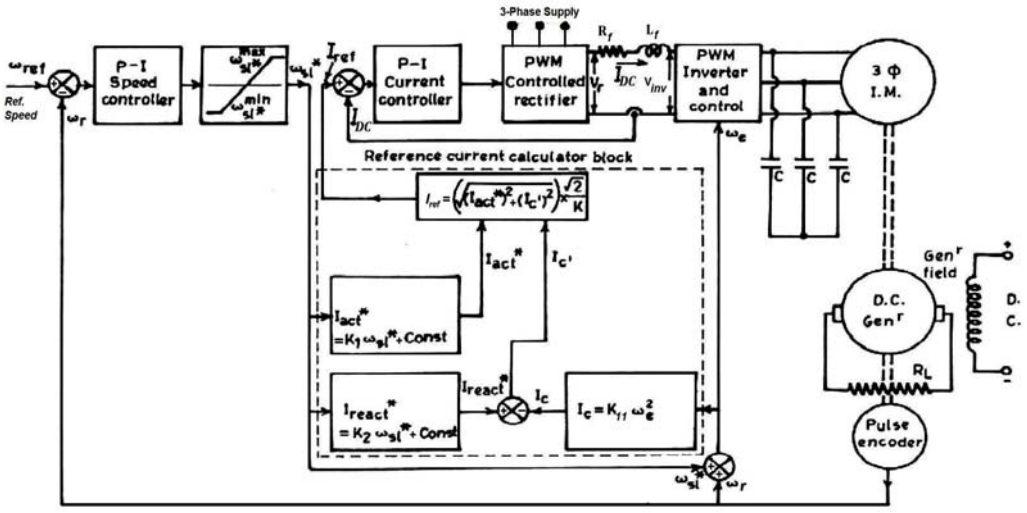

Fig. 1: Variable speed self-commutating PWM current source inverter fed induction motor drive

$$i_{0s}{}^{e} = 0 \;;\; i_{qs}{}^{e} = kI_{DC} \;;\; i_{ds}{}^{e} = 0 \tag{11}$$

Assuming power loss in the inverter to be negligible, *i.e.*, input power = output power, we can derive the following:

$$V_{inv}I_{inv} = v_{as}i_{as} + v_{bs}i_{bs} + v_{cs}i_{cs} = \frac{3}{2}\left(v_{qs}{}^{e}i_{qs}{}^{e} + v_{ds}{}^{e}i_{ds}{}^{e}\right) \tag{12}$$

Substituting the values of $i_{qs}{}^{e}$, $i_{ds}{}^{e}$, and I_{inv} in terms of I_{DC}, the following equation is obtained:

$$V_{inv} = 1.5\,k\,v_{qs}{}^{e} \tag{13}$$

C. DC link

The rectifier output voltage V_r is the sum of the inverter input voltage V_{inv} and DC link voltage, hence

$$V_r = 1.5\,k\,V_{qs}{}^{e} + \left(R_f + pL_f\right)I_{DC} \tag{14}$$

D. Three-phase induction motor with load

The induction motor can be modeled in the d^e-q^e reference frame using the following assumptions:

- The three-phase stator windings of the motor are balanced and sinusoidally distributed in space.
- The air gap flux is maintained at rated value.
- The motor line currents are sinusoidal due to capacitor at the motor terminals.
- The DC link current is ripple free.
- The inverter switching transients are ignored.
- There is no core loss in the motor.

The motor can be described by fourth-order matrix equation in d^e-q^e reference frame as follows:

$$\begin{bmatrix} v_{qs}^{e} \\ v_{ds}^{e} \\ 0 \\ 0 \end{bmatrix} = \begin{bmatrix} R_s + pL_s & \omega_e L_s & pL_m & \omega_e L_m \\ -\omega_e L_s & R_s + pL_s & -\omega_e L_m & pL_m \\ pL_m & \omega_{sl} L_m & R_r + pL_r & \omega_{sl} L_r \\ -\omega_{sl} L_m & pL_m & -\omega_{sl} L_r & R_r + pL_r \end{bmatrix} \begin{bmatrix} i_{qs}^{e} \\ i_{ds}^{e} \\ i_{qr}^{e} \\ i_{dr}^{e} \end{bmatrix} \tag{15}$$

The electromagnetic torque equation of the motor is expressed as follows:

$$T_e = \frac{3}{2}.\frac{P}{2}.L_m\left(i_{qs}{}^{e}i_{dr}{}^{e} - i_{qr}{}^{e}i_{ds}{}^{e}\right) \tag{16}$$

The equation of motion of the drive is given by the following:

$$T_e = T_l + J\frac{d\omega_r}{dt} + B\omega_r \tag{17}$$

The load torque equation is expressed as

$$T_l = T_L.\left(\omega_r/\omega_{base}\right) \tag{18}$$

E. Three-phase capacitor bank

The capacitor current is related to the stator voltage of the induction motor, as shown below:

$$i_c = C\frac{dv_s}{dt} \tag{19}$$

Transforming (19) in the synchronously rotating reference frame d^e-q^e, we have the following:

$$\left(i_{dc}^{e}\cos\omega_e t - i_{qc}^{e}\sin\omega_e t\right) = C\frac{d}{dt}\left(v_{ds}^{e}\cos\omega_e t - v_{qs}^{e}\sin\omega_e t\right) \tag{20}$$

Differentiating (20) and comparing the terms on both sides, *d*-axis and *q*-axis currents are expressed as follows:

$$i_{dc}^{e} = C\left(pv_{ds}^{e} - \omega_e v_{qs}^{e}\right) \tag{21}$$

$$i_{qc}^{e} = C\left(pv_{qs}^{e} + \omega_e v_{ds}^{e}\right) \tag{22}$$

IV. Dynamic Performance Analysis

A three-phase capacitor bank of 150 µF per phase is preferred at the motor terminals for the near sinusoidal current over a wide range of operating frequency [6]. The dynamic performance of the drive is investigated through MATLAB simulation by implementing the designed values of regulator parameters and using the mathematical model of the drive along with analyzing the current and speed transient responses of the drive for the following cases:

1. Start-up
2. Decrease in load torque
3. Increase in load torque
4. Speed deceleration
5. Speed acceleration
6. Speed acceleration and decrease in load torque
7. Speed deceleration and increase in load torque
8. Speed deceleration and decrease in load torque
9. Speed acceleration and increase in load torque
10. Speed reversal

The current and speed responses of the drive employing aforesaid transient conditions one by one each after an interval of 10 seconds are shown in Figure 2. However, the dynamic performance of the drive can be analyzed well by considering the speed and current responses of the drive separately for each transient condition as depicted in Figures 3-4.

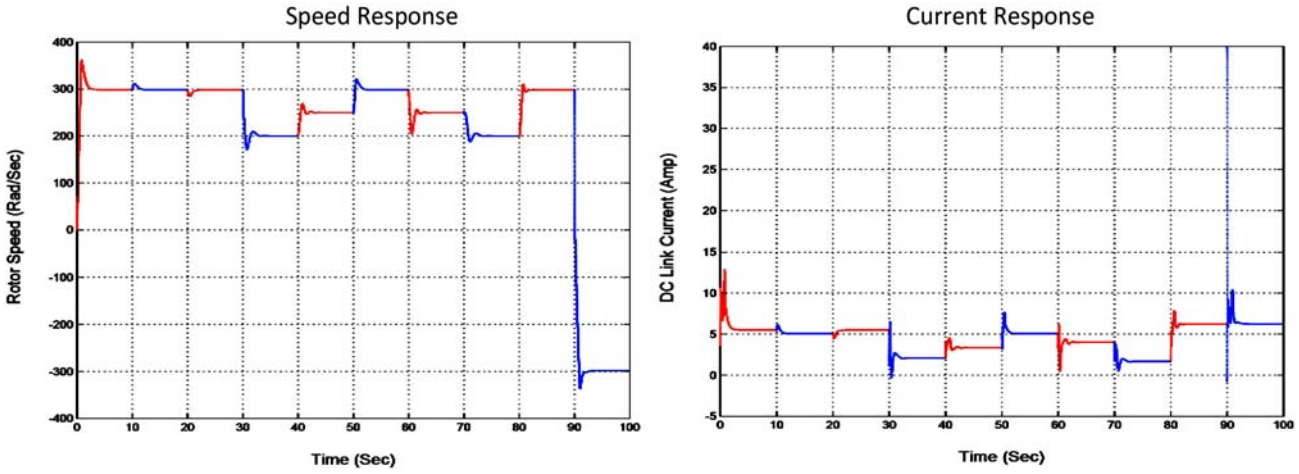

Fig. 2: Speed and current responses of the drive employing different transient conditions each after an interval of 10 seconds.

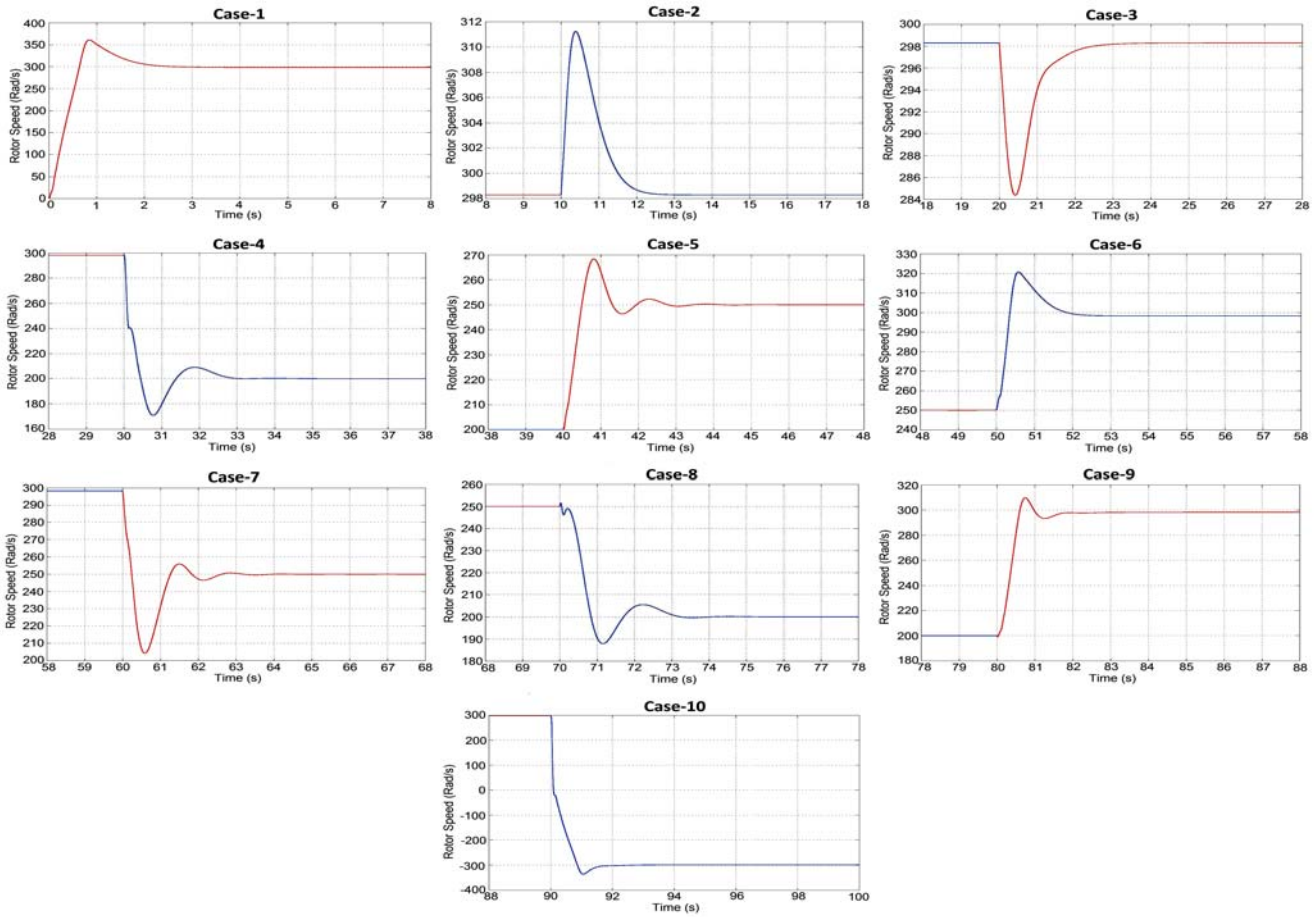

Fig. 3: Speed responses of the drive separately for each transient case.

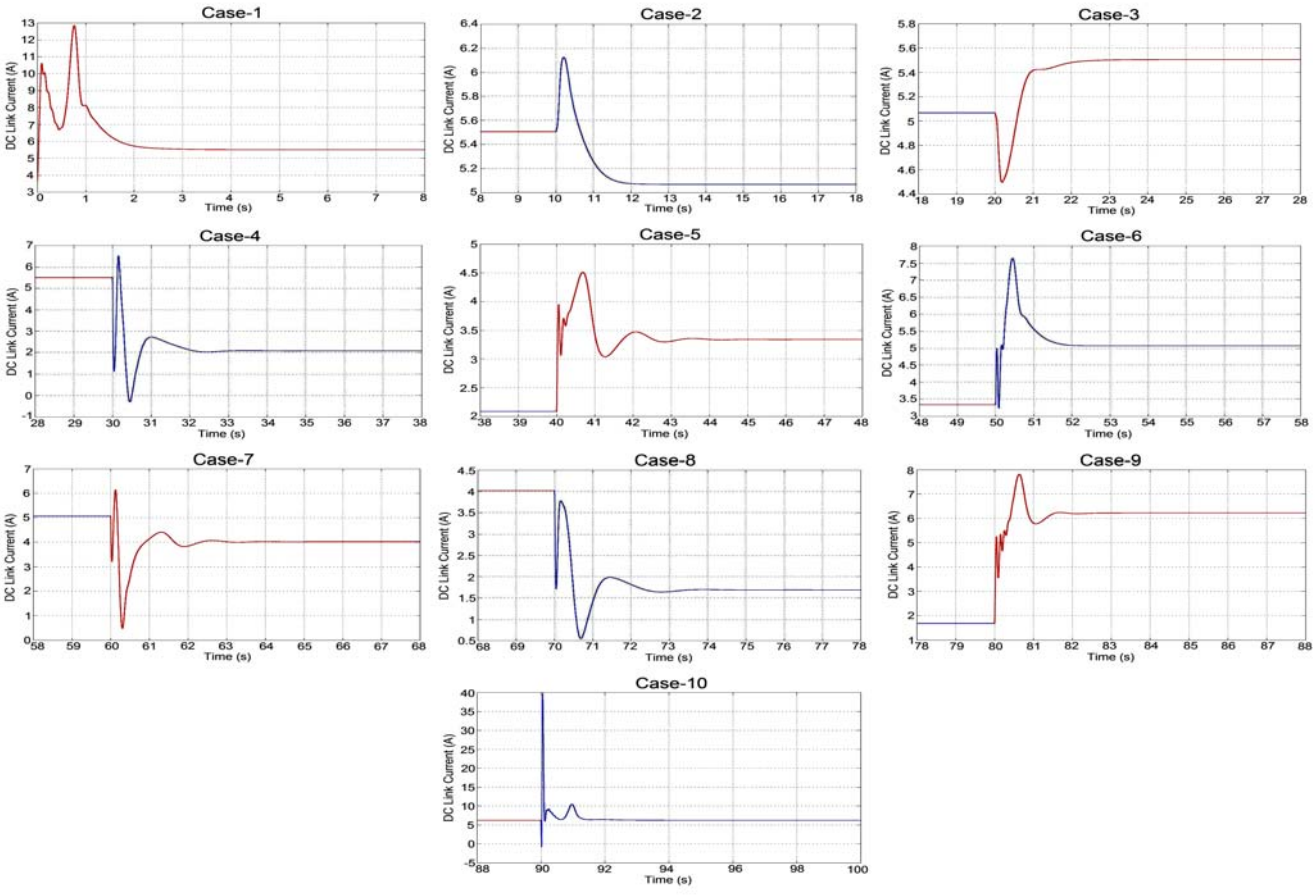

Fig. 4: Current responses of the drive separately for each transient case.

Case–1: Start-up

Initially the motor is at stand still. A step speed command of rated value (298.29 rad/s) from standstill is furnished. Speed PI regulator sets the speed of the rotor at the reference speed selected without exceeding the permissible over shoot limit of the speed in 3.24 seconds as depicted in Figure 3 (case-1). The DC link current corresponding to rotor speed (298.29 rad/s) and load torque (1.31 N-m) is realized 5.506 A as shown in Figure 4 (case-1).

Case–2: Decrease in load torque

The load torque on the motor running at 298.29 rad/s is reduced to 1.00 N-m immediately after 10 seconds and as a result the rotor speed tends to increase but it again settles to 298.29 rad/s in 3.19 seconds as depicted in Figure 3 (case-2). The steady-state value of the DC link current corresponding to rotor speed (298.29 rad/s) and load torque (1.00 N-m) decreases to 5.068 A as shown in Figure 4 (case-2).

Case–3: Increase in load torque

The load torque on the motor running at 298.29 rad/s is now increased to 1.31 N-m immediately after 20 seconds and as a result the rotor speed tends to decrease but it again settles to 298.29 rad/s in 3.21 seconds as shown in Figure 3 (case-3).
It can be observed from Figure 4 (case-3) that the DC link current corresponding to rotor speed (298.29 rad/s) and load torque (1.31 N-m) acquires the same steady-state value (5.506 A) as in the case-1.

Case–4: Speed deceleration

The reference speed of the motor running at 298.29 rad/s is changed to 200 rad/s immediately after 30 seconds and the motor in turn starts decelerating and settles to 200 rad/s in 3.17 sec. as shown in Figure 3 (case-4). The steady-state value of the DC link current corresponding to rotor speed (200 rad/s) and load torque (1.31 N-m) decreases to 2.087 A as depicted in Figure 4 (case-4).

Case–5: Speed acceleration

The reference speed of the motor running at 200 rad/s is changed to 250 rad/s immediately after 40 seconds and the motor in turn starts accelerating and settles to 250 rad/s in 3.69 seconds as shown in Figure 3 (case-5).
The steady-state value of the DC link current corresponding to rotor speed (250 rad/s) and load torque (1.31 N-m) increases to 3.340 A as depicted in Figure 4 (case-5).

Case–6: Speed acceleration and decrease in load torque

The reference speed of the motor running at 250 rad/s is changed to 298.29 rad/s and the load torque on the motor is decreased to 1.00 N-m together immediately after 50 seconds and as a result the rotor speed starts accelerating and it settles to 298.29 rad/s in 2.87 seconds as depicted in Figure 3 (case-6).
It can be observed from Figure 4 (case-6) that the DC link current corresponding to rotor speed (298.29 rad/s) and load torque (1.00 N-m) acquires the same steady-state value (5.068 A) as in the case–2.

Case–7: Speed deceleration and increase in load torque

The reference speed of the motor running at 298.29 rad/s is changed to 250 rad/s and the load torque on the motor is increased to 1.85 N-m together immediately after 60 seconds and as a result the rotor speed starts decelerating and it settles to 250 rad/s in 3.65 seconds as depicted in Figure 3 (case-7). It can be observed from Figure 4 (case-7) that the steady-state value of the DC link current corresponding to rotor speed (250 rad/s) and load torque (1.85 N-m) decreases to 4.023 A, though this value is higher than the steady-state value of case–5 on account of increased load torque.

Case–8: Speed deceleration and decrease in load torque

The reference speed of the motor running at 250 rad/s is changed to 200 rad/s and the load torque on the motor is decreased to 1.00 N-m together immediately after 70 seconds and as a result the rotor speed starts decelerating with an early swing and it settles to 200 rad/s in 3.43 seconds as depicted in Figure 3 (case-8). It can be observed from Figure 4 (case-8) that the DC link current corresponding to rotor speed (200 rad/s) and load torque (1.00 N-m) decreases to 1.689 A, which is lower than the steady-state value of case–4 on account of decreased load torque.

Case–9: Speed acceleration and increase in load torque

The reference speed of the motor running at 200 rad/s is changed to 298.29 rad/s and the load torque on the motor is increased to 1.85 N-m together immediately after 80 seconds and as a result the rotor speed starts accelerating with a relatively tiny early swing and it settles to 298.29 rad/s in 3.02 seconds as depicted in Figure 3 (case-9). It can be observed from Figure 4 (case-9) that the DC link current corresponding to rotor speed (298.29 rad/s) and load torque (1.85 N-m) increases to 6.230 A, which is the highest among the steady-state values of the cases – 1, 2, 3 and 6 on account of very high load torque.

Case–10: Speed reversal

Figure 3 (case-10) shows the response of the motor drive to the reversal of speed. The motor is running stably at positive set reference speed of rated value (298.29 rad/s) and immediately after 90 seconds the set speed is changed to -298.29 rad/s. In response to this change, the speed regulator is actuated and the drive system control structure implements the braking at controlled frequencies followed by its reverse motoring up to the set reference speed in 3.84 seconds. It can be seen from Figure 4 (case-10) that the DC link current corresponding to rotor speed (-298.29 rad/s) and load torque (1.85 N-m) attains the previous steady-state value (6.230 A).

As summarized in Table-1, the DC link current and drive settling time corresponding to different transient conditions stated aforesaid, it is found that the steady-state value of the DC link current is increased / decreased with increase / decrease in motor speed and / or in load torque. The speed PI regulator maintains the speed to its set reference value for variation in the load torque within the prescribed limit. The speed settling takes place in the time duration 2.87-3.84 seconds. The dynamic performance

curves and facts in Table-1 show the effectiveness of speed and current PI regulators.

Table-1: Summary of different cases

Case	Step-change in Reference Speed (rad/s)		Step-change in Load Torque (N-m)		DC Link Current (A)	Drive Settling Time (s)
	From	To	From	To		
1	0	298.29	1.31		5.506	3.24
2	298.29		1.31	1.00	5.068	3.19
3	298.29		1.00	1.31	5.506	3.21
4	298.29	200	1.31		2.087	3.17
5	200	250	1.31		3.340	3.69
6	250	298.29	1.31	1.00	5.068	2.87
7	298.29	250	1.00	1.85	4.023	3.65
8	250	200	1.85	1.00	1.689	3.43
9	200	298.29	1.00	1.85	6.230	3.02
10	298.29	-298.29	1.85		6.230	3.84

V. CONCLUSIONS

A closed-loop scheme incorporating speed and current PI regulators of the V/Hz controlled PWM self-commutating CSI-fed induction motor drive has been discussed. A mathematical model of the induction motor drive has been developed by considering different sections of the model to investigate the dynamic performance of the drive system. The exploration of the dynamic response curves obtained through MATLAB simulation has confirmed that the control structure of the drive takes care of transients in a proper time. It is also observed that the level of the transient current never exceeds the permissible value. Therefore, it is concluded that the motor control scheme takes care of the over current of the inverter devices. The proposed scheme has confirmed that there are quick and instantaneous changes in the DC link currents in accordance with any disturbances in the reference speed / load torque thereby provides fast response of the drive system.

APPENDIX

Name plate ratings of induction motor

1 hp, three-phase, 400 V, 50 Hz, 4-pole, 1425 rpm, star

Induction motor parameters

R_s = 3.520 Ω R_r = 2.780 Ω L_s = 0.165 H
L_r = 0.165 H L_m = 0.150 H J = 0.01289 kg-m^2

DC link parameters

R_f = 0.250 Ω, L_f = 0.040 H

REFERENCES

[1] P. Agarwal and V. K. Verma, "Performance Evaluation of Current Source Inverter-fed Induction Motor Drive", Journals of Institution of Engineers, Vol.72, pp. 209-217, February 1992.

[2] P.N. Enjeti, P.D. Ziogas and J.F. Lindsay, "Programmed PWM Technique to Eliminate Harmonics: A Critical Evaluation", IEEE Transactions on Industry Applications, Vol. 26, No. 2, pp. 302-315, March/April 1990.

[3] S.R. Bowes and R.I. Bullough, "Optimal PWM Microprocessor Controlled Current Source Inverter Drives", IEEE Proceedings, Vol. 135, Pt. B, No. 2, pp. 59-75, March 1988.

[4] Y. Xiao, B. Wu, S. Rizzo and R. Sotuden, "A Novel Power Factor Control Scheme for High Power GTO Current Source Converter", Conference Record IEEE-IAS, pp. 865-869, 1996.

[5] A.K. Pandey and S.M. Tripathi, "Determination of Regulator Parameters and Transient Analysis of Modified Self-commutating CSI-fed IM Drive", Journal of Electrical Engineering and Technology, Korean Institute of Electrical Engineers, Vol. 6, No. 1, pp. 48-58, January 2011.

[6] A.K. Pandey, Pramod Agarwal and V.K. Verma, "Optimal Capacitor Selection for Modified Self-commutated CSI-fed Induction Motor Drive", IEEE ISIE 2006, Montreal, Quebec, Canada, pp. 1166-1171, July 9-12, 2006.

[7] P. Agarwal and V.K. Verma, "Parameter Coordination of Microcomputer Controlled CSI-fed Induction Motor Drive", IE (I) Journal – EL, Vol. 88, pp. 25-34, December 2007.

[8] Pramod Agarwal, V.K. Verma and A.K. Pandey, "Performance Evaluation of a Self-commutating CSI-fed Induction Motor Drive for Different Operating Conditions, IETE Journal of Research, Vol. 54, Issue 4, pp. 227-238, July/Aug. 2008.

[9] Pramod Agarwal, A.K. Pandey and V.K. Verma, "Performance Investigation of Modified Self-commutated CSI-fed Induction Motor Drive, Asian Power Electronics Journal, Vol. 3, No. 1, pp. 21-29, Sept 2009.

BIOGRAPHIES

Saurabh Mani Tripathi is presently working as Assistant Professor of Electrical Engineering at Kamla Nehru Institute of Technology, Sultanpur, (U.P.), India. He obtained his B.Tech. degree in Electrical and Electronics Engineering in 2006 and did his M.Tech. in Power Electronics and Drives in 2009 from U.P. Technical University, Lucknow. He has published several research papers and authored several books on modern control system and basic system analysis. His areas of interest include electrical machines, control systems, power electronics, and electric drives.

Ashok Kumar Pandey received his Ph.D. degree in Electrical Engineering from Indian Institute of Technology, Roorkee in 2003. He did his M.Tech. in Power Electronics, Electrical Machines and Drives from Indian Institute of Technology, Delhi in 1995. Currently, he is working as an Associate Professor with the Department of Electrical Engineering at M.M.M. Engineering College, Gorakhpur, (U.P.), India. His areas of interest include power electronics, electrical machines, and drives. He is a fellow of Institution of Engineers (IE), India and Institution of Electronics and Telecommunication Engineers (IETE), India.